University of Groningen

Low-temperature gaseous nitriding and subsequent oxidation of epitaxial Ni/Fe bilayers

Mijiritskii, A.V.; Boerma, D.O

IMPORTANT NOTE: You are advised to consult the publisher's version (publisher's PDF) if you wish to cite from it. Please check the document version below.

Document Version
Publisher's PDF, also known as Version of record

Link to publication in University of Groningen/UMCG research database

Low-temperature gaseous nitriding and subsequent oxidation of epitaxial Ni/Fe bilayers

A. V. Mijiritskii, and D. O. Boerma

Low-temperature gaseous nitriding and subsequent oxidation of epitaxial Ni/Fe bilayers

A. V. Mijiritskii[a)] and D. O. Boerma
Nuclear Solid State Physics, Materials Science Centre, University of Groningen, 9747 AG Groningen, The Netherlands

Low-temperature gaseous nitriding was applied to epitaxial Ni/Fe bilayers deposited onto a MgO(001) substrate. The pore-free nitride layers produced were subsequently oxidized in oxygen. The samples were analyzed by conversion electron Mössbauer spectroscopy (CEMS), x-ray diffraction (XRD), and Rutherford backscattering spectroscopy in combination with channeling techniques. Nitriding in pure NH_3 gas at 300 °C led to the formation of a textured ϵ-Fe–nitride layer with a predominant composition of $Fe_{2.07}N$. The epitaxial relationship of the ϵ-Fe–nitride layer with the MgO substrate was found to be ϵ-$Fe_{2.07}N\{203\}\langle010\rangle\|MgO\{001\}\langle110\rangle$. The nitride layer produced was subsequently oxidized in $p(O_2) = 100$ mbar at 275 °C. While the XRD spectra acquired on the oxidized samples revealed the formation of a Fe–oxide phase with a spinel structure, the CEMS spectral lines could not be interpreted in terms of any Fe–oxide or Fe–hydroxide phase know. It is suggested that the peculiarities in the CEMS data are caused by N atoms incorporated into the oxide lattice. © *2000 American Vacuum Society.* [S0734-2101(00)13704-2]

I. INTRODUCTION

Thin layers of Fe–nitrides and Fe–oxides are of interest due to their magnetic properties.[1–3] Unfortunately, in many cases the possible application of these materials is hindered by technological difficulties in their production.

From a technological point of view, one of the most attractive ways to form Fe–nitrides is gaseous nitriding of Fe in a $NH_3 + H_2$ mixture. The disadvantage of this method is the necessity to apply relatively high (above 500 °C) temperatures upon the nitriding. Such high temperatures lead to the formation of pores in the layers due to partial decomposition of the thermodynamically unstable Fe–nitrides into $Fe + N_2$ during this nitriding process. Recently, we have found a method allowing fabrication of Fe–N phases in a mixture of $NH_3 + H_2$ at relatively low temperatures (275–350 °C) by using a Ni cap layer as a catalyst.[4,5] With this method pore-free Fe–nitride layers can be obtained. The role of the Ni cap layer has been found to be twofold: (i) it promotes decomposition of the NH_3 molecules into atomic N and H; (ii) it protects the underlying Fe layer from possible oxidation by a small amount of H_2O often present in the system. It was found that H_2O desorbs from the walls of the system after letting in NH_3 gas. In the present work, as well as in our previous study,[4] it was determined that no Fe oxidation occurs during nitriding in $NH_3 + H_2$ mixtures at 1000 mbar when the cap layer has a thickness of 25 nm or more. During nitriding the native NiO on the Ni cap layer is reduced to metallic Ni. In this, and also in earlier work of our group,[4,6] it was determined that no interdiffusion of Ni and Fe takes place during prolonged vacuum annealing of Ni/Fe bilayers at temperatures below 325 °C. This observation is in agreement with a number of studies on Ni–Fe interdiffusion.[7–9]

We applied this method to a Ni/Fe bilayer grown epitaxially on MgO and found that α''-, γ'-, and ϵ-Fe–nitride phases can be formed, depending on the nitriding potential of the $NH_3 + H_2$ mixture and the temperature.

Only a few publications exist on gaseous oxidation of Fe–nitrides. No clear evidence of the formation of oxynitrides has been reported.[10–13]

In this article we discuss the formation and subsequent low-temperature oxidation of ϵ-Fe–nitride.

II. EXPERIMENTAL DETAILS

A MgO single crystal was cleaved in air along a (100) plane. Prior to the Ni/Fe deposition the substrate was annealed in vacuum (starting base pressure 5×10^{-10} mbar) at a temperature of about 600 °C for several hours to remove adsorbates and surface imperfections. The epitaxial Ni/Fe bilayers were grown on MgO(100) by laser ablation deposition (LAD) using a YAG:Nd^{3+} laser ($\lambda = 1.06 \mu$m) with an output energy of 250 mJ, operating in the Q-switched regime ($\tau = 15$ ns) with a repetition rate of 50 Hz. The material was ablated from ^{57}Fe and Ni targets mounted in an ultrahigh vacuum chamber, at a constant rate and constant energy distribution of the atoms in the laser plume. The deposition rate was monitored by an oscillating quartz crystal. The thicknesses of the ^{57}Fe and Ni layers were 100 and 25 nm, respectively. After deposition the samples were transported to other (vacuum) systems for nitriding, oxidation and analysis with x-ray diffraction (XRD), Rutherford backscattering analysis (RBS)/channeling, and conversion electron Mössbauer spectroscopy (CEMS).

Gaseous nitriding was performed in a N furnace made of Pyrex glass. No metal parts were used in the heated part of the furnace. To ensure a constant gas composition at the

[a)]Author to whom correspondence should be addressed; electronic mail: a.mijiritskii@phys.rug.nl

sample surface, gas circulation was created by thermal convection. Prior to the nitriding, the furnace was flushed with NH_3. To produce the ϵ-Fe–nitride phase, the Ni/Fe bilayers were nitrided in pure NH_3 (99.995%) at 300 °C for more than 15 h.

Gaseous oxidation of the Ni/Fe–N system was performed in a specially developed oxygen-resistant oven with a base pressure of 1×10^{-10} mbar.[14] The oxidation was done in $p(O_2) = 100$ mbar at 275 °C for 100 h.

The XRD measurements were carried out in a Philips X'Pert-MRD system and in a conventional Philips XRD system using Cu K_α radiation. Both specular and off-specular geometries were utilized to analyze the sample structure.

In RBS/channeling, a 1 MeV He$^+$ beam was used. The backscattered particles were detected at an angle of 165°. The sample to be investigated was mounted on a three-axis goniometer with a long-range reproducibility and accuracy of better than 0.1°. The orientation of the samples was established by performing RBS/channeling on a bare part of the MgO substrate.

The velocity of the CEMS radioactive source was calibrated by acquiring a spectrum on as-deposited Ni/^{57}Fe/MgO before the sample was subjected to any treatment.

III. RESULTS AND DISCUSSION

The LAD deposited Ni/Fe bilayers were found to be of high crystalline quality with sharp interfaces as revealed by RBS/channeling and XRD measurements. While the Fe layer was found to be single crystalline, the Ni cap layer consisted of two pairs of mutually perpendicular domains with an fcc Ni{110}⟨211⟩ ∥ bcc Fe{100}⟨110⟩∥MgO{100}⟨010⟩ overall epitaxial relationship, as was previously reported.[15]

By low-temperature gaseous nitriding of the Ni/Fe system we succeeded in producing pore-free α''-, γ'-, and ϵ-Fe–nitrides. Which Fe–nitride is formed at a given temperature depends on the nitriding potential r_N. The so-called Lehrer diagram gives boundaries in the r_N/T plane separating regions where a certain phase is formed.[16] The nitriding potential is given by $r_N = p_{NH_3}/p_{H_2}^{3/2}$, where p_{NH_3} and p_{H_2} are partial pressures of NH_3 and H_2 (in Pa) in the $NH_3 + H_2$ mixture. To produce the γ' or ϵ nitride phases in epitaxial layers we found that a higher nitriding potential was needed than to produce the same phases in Ni-covered polycrystalline layers. The formation of nitride phases at low temperatures in Ni-capped polycrystalline Fe layers has been extensively studied in our group.[17] This study has led to an extention of the Lehrer diagram to the 240–350 °C temperature range. For instance, in the present work we found that in epitaxial Fe layers pure γ'-Fe–nitride was formed after nitriding at 300 °C for 9.5 h at $\ln(r_N) = -2.0$. According to the Lehrer diagram pure ϵ-Fe–nitride should be formed under these conditions. In the study[17] of the Lehrer diagram it has been found that indeed a Ni-capped polycrystalline Fe layer of comparable thickness is transformed into pure ϵ-Fe–nitride in just 2.5 h at the same temperature and nitriding potential. Note that the Lehrer diagram represents the Fe–N phases in thermodynamic equilibrium, and in no way reflects the
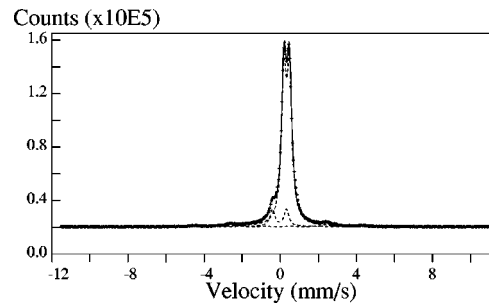

FIG. 1. CEMS spectrum acquired after nitriding of Ni/^{57}Fe/MgO in pure NH_3 at 300 °C. The measured points are indicated by crosses; the solid line is the fit to the spectrum; the dashed lines represent the components of the fit. The values of the hyperfine parameters of the two major components are listed in Table I.

ability to overcome energy barriers for phase transformations. Therefore, the delay observed in the phase formation must be due to the kinetics of the process, and is probably caused by a lack of nucleation sites (such as grain boundaries or lattice defects) in the epitaxial Fe layer.

Gaseous nitriding of an epitaxial Ni/Fe bilayer in pure NH_3 at 300 °C resulted in ϵ-Fe–nitride formation. Typical CEMS and XRD spectra of such a sample are presented in Figs. 1 and 2(a), respectively. The general shape of the CEMS spectrum indicates that the composition of the Fe–nitride formed in the major part of the Fe layer is close to
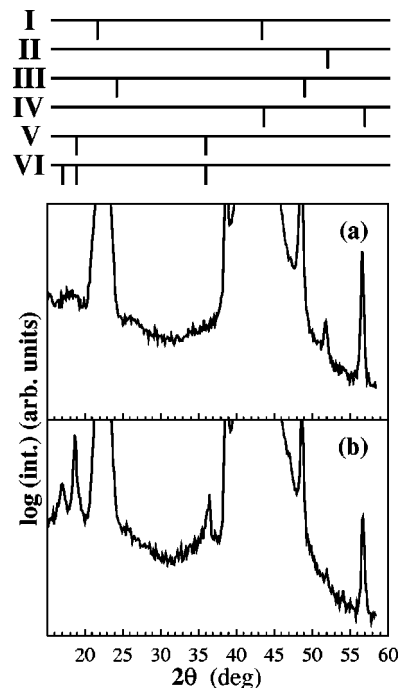
FIG. 2. XRD spectra: (a) after nitriding of Ni/Fe/MgO in pure NH_3 at 300 °C; (b) after oxidation of Ni/ϵ-Fe$_{2.07}$N/MgO in pure O_2 at 275 °C. The bar diagram explains the peak positions observed for: (I) MgO, (II) Ni, (III) Ni$_4$N, (IV) ϵ-Fe$_{2.07}$N, (V) Fe$_3$O$_4$, (VI) γ-Fe$_2$O$_3$, respectively. The sharp peak at about 39° is a MgO(200) reflection due to the K_β radiation of the x-ray source. The observed decrease of the Ni peak at 51.9° is probably due to partial oxidation of Ni. The corresponding NiO reflection is not visible since it nearly coincides with the MgO peak at about 43°.

TABLE I. Hyperfine parameters of the major components obtained from the analysis of the CEMS data for Ni/ϵ-Fe–N/MgO.

Component	I.S. (mm/s)	H.F. (T)	Q.S. (mm/s)	Rel. area (%)
I	0.43 ± 0.01	—	0.29 ± 0.01	86.3 ± 0.1
II	0.06 ± 0.01	—	0.74 ± 0.01	10.1 ± 0.1

Fe_2N.[18] This is in agreement with the XRD measurements and is supported by low-temperature Mössbauer measurements (not shown) where no magnetic splitting of the doublets was found at a temperature of about 80 K. This is expected for ϵ-Fe–nitrides with high nitrogen concentration. Our analysis showed that the CEMS spectrum taken at room temperature (RT) consists of two quadrupole-split doublets plus a weak magnetically split component. The magnetic field experienced by the Fe atoms, causing magnetic splitting in the spectra, has a broad distribution up to B fields of about 27 T. To include this distribution, in our analysis we fit the magnetically split component with two broad sextets. The magnetically split component takes only 3.6% of the total spectral area. The hyperfine parameters calculated for the major components are presented in Table I. The two quadrupole-split doublets point to the presence of two different Fe sites and therefore to a deviation from the exact Fe_2N composition. The areas of the doublets reflect the probabilities of the different Fe sites. On the basis of the nitrogen ordering model proposed by Jack,[19] we obtained the composition of $Fe_{2.07}N$ from the ratio of the doublet areas. The small total spectral area covered by magnetically split sextets may be caused by ferromagnetic ϵ-Fe–nitride phases which have a Curie temperature above RT. The Curie temperature is a function of the N concentration. Fe_xN phases with $x \geq 2.2$ are ferromagnetic at RT. In our CEMS spectrum, the main component (86.3%) has an isomer shift and a quadrupole splitting that are, within the error bars, the same as those found by Schaaf et al.[18] Like Schaaf, we found a second, weaker nonmagnetic component (10.1% in our case). However the isomer shift and the quadrupole splitting we determined for this component are different from the values reported by Schaaf. The shift in the position of this second component is clearly visible as a shoulder in the shape of the CEMS spectrum. The shift is too large to be interpreted by strain in the lattice. We have no explanation for this observation.

Apart from the XRD peaks caused by the reflections from the MgO substrate and the Ni cap layer, all peaks in the scan presented in Fig. 2(a) can be attributed to ϵ-Fe–nitride. This also applies to the spectrum from 60° to 125° (not shown).

Extended XRD studies of the sample revealed that the ϵ-Fe–nitride formed upon nitriding of the Ni/Fe/MgO system is highly textured. Utilizing both specular and off-specular geometries, it was found that the ϵ-$Fe_{2.07}N$ layer consists of 12 structural domains with an epitaxial relationship as ϵ-$Fe_{2.07}N\{203\}\langle010\rangle\|MgO\{001\}\langle110\rangle$. The details of the transformation leading to this epitaxial relationship will be discussed elsewhere.[20]
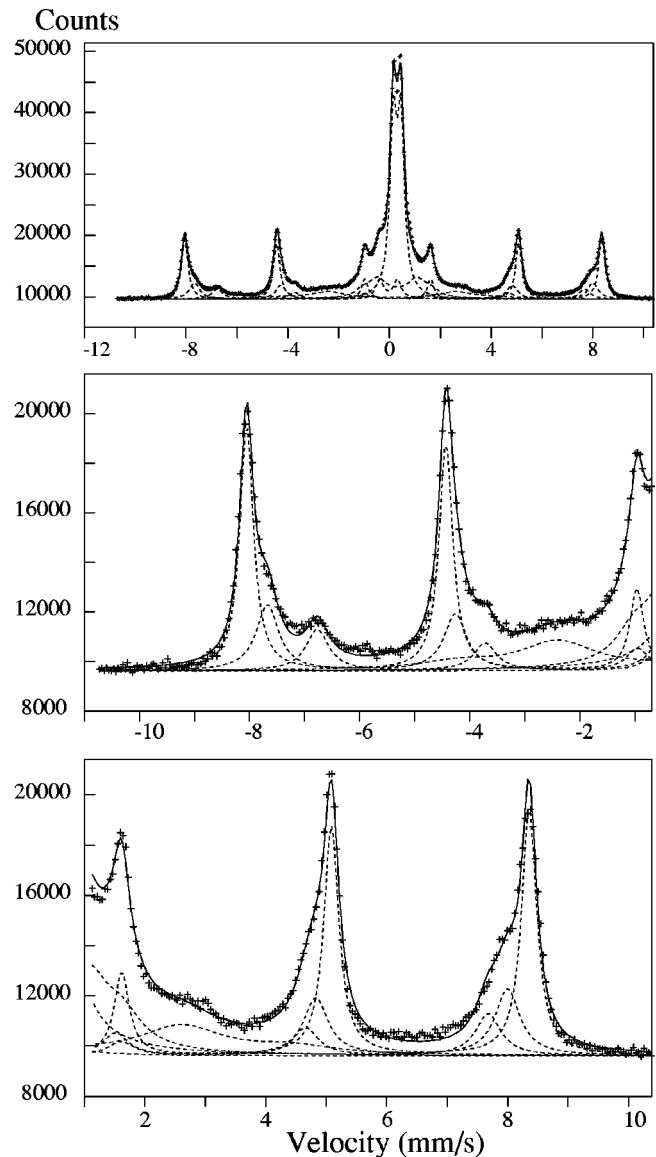

FIG. 3. CEMS spectrum acquired after oxidation of Ni/ϵ-$^{57}Fe_{2.07}N$/MgO in pure O_2 at 275 °C. The measured points are indicated by crosses; the solid line is the fit to the spectrum; the dashed lines represent the components of the fit. The values of the hyperfine parameters of the oxidic components are listed in Table II.

XRD and CEMS spectra acquired after low-temperature oxidation of the Ni/ϵ-$Fe_{2.07}N$/MgO system for 100 h are presented in Figs. 2(b) and 3, respectively. The formation of Fe–oxide is evident from both spectra. According to the CEMS data, approximately 44% of Fe of the ϵ nitride was converted into the oxidic state. Light microscopy (LM) and scanning electron microscopy (SEM) analysis performed on oxidized samples revealed a high density of blisters ranging in size from 1 to 100 μm. We also observed some holes and debris, apparently due to the bursting of blisters. With this morphology a reliable determination of the composition of the oxide layer formed is impossible with RBS. Therefore, we have no information on the oxygen content in the layers or whether the oxide is formed at the Ni/Fe–N interface or throughout the whole Fe–N layer. The positions of the ob-

TABLE II. Hyperfine parameters of the oxidic components obtained from the analysis of the CEMS data for oxidized Ni/Fe–N–O/MgO.

Component	I.S. (mm/s)	H.F. (T)	Q.S. (mm/s)	Rel. area (%)
I	0.343 ± 0.002	50.88 ± 0.02	-0.174 ± 0.003	59.6 ± 0.1
II	0.327 ± 0.008	48.6 ± 0.1	-0.12 ± 0.02	25.6 ± 0.1
III	0.57 ± 0.02	44.80 ± 0.09	-0.01 ± 0.03	14.8 ± 0.1

served peaks in the XRD spectrum are very close to γ-Fe_2O_3. Note, that with this interpretation the peak at about $17°$ is due to ordering of Fe vacancies in $Fe_{3-\delta}O_4$. Here, γ-Fe_2O_3 is modelled as $Fe_{3-\delta}O_4$, with $\delta = 0.3$.[21] The set of the diffraction peaks could also be attributed to a mixture of γ-Fe_2O_3 and Fe_3O_4. In the CEMS spectra, the observed magnetic splittings and isomer shifts are typical for Fe–oxides. However, as will be discussed below, the particular combination of isomer shifts, electric quadrupole splittings and magnetic splittings observed for the major components in the CEMS spectra cannot be explained by either of these phases or by their mixture.

Extensive studies on oxidation of ϵ-Fe–nitrides have been published lately by Kooi *et al.* and Graat *et al.*[10–12,22] Depending on the oxidation conditions, the authors reported the formation of Fe_3O_4, α-Fe_2O_3, and $Fe_{1-x}O$ oxide phases. In our case, CEMS and XRD measurements did not reveal either α-Fe_2O_3 or $Fe_{1-x}O$ phase formation.

The parameters of the CEMS spectrum (Fig. 3) are listed in Table II. The lines appearing after oxidation can be fitted with three components. The magnetic fields of the components indicate unambiguously that the Fe atoms of the material produced are in oxidic surrounding. The hyperfine parameters of the first component are in the range between the parameters expected for γ-Fe_2O_3 and α-Fe_2O_3. This points to the fact that the corresponding Fe is in the $3+$ oxidation state. Since on the one hand it is the largest component of the three and on the other hand no trace of α-Fe_2O_3 is visible in the XRD spectra, the Fe^{3+} ions giving rise to the first component probably form a spinel structure.

At first sight, the second component could be ascribed to the tetrahedral A site (Fe^{3+}) of Fe_3O_4. However, the quadrupole splitting of this second component is far too big for such an interpretation. This component cannot be ascribed to the α-Fe_2O_3 phase either because there is a large discrepancy in the magnetic hyperfine field and in the isomer shift. Also, there is no trace of α-Fe_2O_3 in the XRD spectra.

The third component has an isomer shift typical for the octahedral B site in Fe_3O_4, corresponding to the $Fe^{2.5+}$ charge state. The magnetic splitting and the low quadrupole splitting of this component are also in agreement with such an identification. It is possible that the component corresponding to the A site (with an intensity of 0.5 times the intensity of the B site for stoichiometric Fe_3O_4) is also present in our CEMS spectra.

Summarizing, the origin of the two strongest components in the Fe–oxide part of our CEMS spectra cannot be interpreted in terms of lines due to known Fe–oxides. The observed line positions can also not be identified with Fe–oxyhydrides. We propose that the first and the second components are due to an Fe–oxide with a spinel structure, containing N atoms incorporated into the lattice.

The information on Fe–oxynitrides is very scarce. Kooi *et al.*[10] and Graat *et al.*[11,12,22] have studied gaseous oxidation of a layer of ϵ-Fe–nitride formed on a thick Fe sample. They observed that N atoms released due to oxidation did not remain in the oxide layer being formed. At oxidation temperatures above $250°C$ the released N atoms were found to diffuse rapidly into the bulk of the remaining Fe–nitride. This resulted in the formation of ϵ-Fe–nitride phases with a higher N concentration. At oxidation temperatures below $150°C$ the released N atoms were found to accumulate beneath the forming Fe–O layer at the Fe–O/Fe–N interface. Since the calculated amount of the nitrogen set free due to Fe oxidation did not correspond to the amount of nitrogen found in the samples after oxidation, the authors suggested that the surplus nitrogen could leave the sample, probably in the form of N_2. After oxidation of our samples we found some blistering indicating that N_2 gas was produced. Nevertheless as argued above, some N may have been incorporated into the Fe–oxide.

Voogt has reported the formation of N-incorporated Fe_3O_4 and $Fe_{1-x}O$ upon NO_2-assisted molecular beam epitaxial growth of Fe–oxide layers.[13] The conclusion was drawn on the basis of x-ray photoelectron spectroscopy, CEMS, and reflection high-energy electron diffraction measurements. The author suggested that the N atoms occupy substitutional sites in the oxygen sublattice. However, their CEMS spectra look entirely different from ours. In addition to two ''normal'' Fe_3O_4 components with no quadrupole splitting, they observe a third component with a lower hyperfine field of about 42 T. From this it is clear that we formed a different compound.

Additional studies are necessary to determine the composition of the Fe–oxynitride produced and to establish the possible existence of ordering of the incorporated N atoms. Also, the magnetic properties of the layers will be studied.

IV. CONCLUSION

Summarizing, low-temperature gaseous nitriding and subsequent oxidation of epitaxial Ni/Fe bilayers was studied. The Ni cap layer served as a catalyst and allowed us to produce pore-free Fe–nitride layers. Upon nitriding, higher values of the nitriding potential had to be used to form a certain Fe–N phase, compared to the values according to the Lehrer diagram. This phenomenon was explained by a lack of nucleation sites in the epitaxial layers. Nitriding in pure NH_3 at $300°C$ resulted in the formation of ϵ-$Fe_{2.07}N$ having a ϵ-$Fe_{2.07}N\{203\}\langle010\rangle \| MgO\{001\}\langle110\rangle$ epitaxial relationship with respect to the MgO substrate. The Fe–oxide phase formed upon low-temperature gaseous oxidation of $Ni/Fe_{2.07}N$ was identified to have a spinel-like structure. The CEMS spectra obtained for this Fe–oxide phase could not be ascribed to any of the Fe–oxide or Fe–hydroxide phases known. It is suggested that the peculiarities in the CEMS

data are caused by N incorporated into the oxide lattice. Further studies are needed for a complete characterization of the compound produced.

ACKNOWLEDGMENTS

[1] S. Wang and M. H. Kryder, J. Appl. Phys. **69**, 5625 (1991).

[2] Z.-J. Wang, L. S. Wen, X.-R. Chang, Y. S. Gu, Zh.-Zh. Tian, and J. M. Xiao, Appl. Phys. Lett. **68**, 2887 (1996).

[3] P. J. H. Bloemen, P. A. A. van der Heijden, R. M. Wolf, J. aan de Stegge, J. T. Kohlhepp, A. Reinders, R. M. Jungblut, P. J. van der Zaag, and W. J. M. de Jonge, Mater. Res. Soc. Symp. Proc. **401**, 485 (1996).

[4] D. K. Inia, W. A. Arnoldbik, A. M. Vredenberg, and D. O. Boerma, Surf. Eng. **12**, 326 (1996).

[5] D. K. Inia, M. H. Pröpper, W. A. Arnoldbik, A. M. Vredenberg, and D. O. Boerma, Appl. Phys. Lett. **70**, 1245 (1997).

[6] D. K. Inia, F. W. J. Feiner, W. M. Arnoldbik, A. M. Vredenberg, and D. O. Boerma, Surf. Coat. Technol. **83**, 65 (1996).

[7] P. R. Munroe and M. Hatherly, Scr. Metall. Mater. **32**, 93 (1995).

[8] R. J. Borg and D. Y. F. Lai, Acta Metall. **11**, 861 (1963).

[9] K. Hirano, M. Cohen, and B. L. Averbach, Acta Metall. **9**, 440 (1961).

[10] B. J. Kooi, M. A. J. Somers, and E. J. Mittemeijer, Thin Solid Films **281/282**, 488 (1996).

[11] P. C. J. Graat, M. A. J. Somers, and E. J. Mittemeijer, Appl. Surf. Sci. **136**, 238 (1998).

[12] P. C. J. Graat, M. A. J. Somers, and E. J. Mittemeijer, Thin Solid Films **340**, 87 (1999).

[13] F. C. Voogt, Ph.D. thesis, Groningen University, 1998.

[14] G. Dorenbos, Ph.D. thesis, Groningen University, 1994.

[15] A. V. Mijiritskii, P. J. M. Smulders, V. Ya. Chumanov, O. C. Rogojanu, M. A. James, and D. O. Boerma, Phys. Rev. B **58**, 8960 (1998).

[16] E. Lehrer, Z. Elektrochem. Angew. Phys. Chem. **36**, 383 (1930).

[17] E. H. du Marchie van Voorthuysen, B. Feddes, N. G. Chechenin, D. K. Inia, A. M. Vredenberg, and D. O. Boerma, Phys. Status Solidi A **177**, 127 (2000).

[18] P. Schaaf, Ch. Illgner, M. Niederdrenk, and K. P. Lieb, Hyperfine Interact. **95**, 199 (1995).

[19] K. H. Jack, Acta Crystallogr. **5**, 404 (1952).

[20] A. V. Mijiritskii *et al.* (unpublished).

[21] R. M. Cornell and U. Schwertmann, *The Iron Oxides* (VCH, New York, 1996).

[22] P. C. J. Graat, H. W. Zandbergen, M. A. J. Somers, and E. J. Mittemeijer Oxid. Met. (submitted).